Available online at www.sciencedirect.com
ScienceDirect
Polymer 48 (2007) 2395–2403
polymer
www.elsevier.com/locate/polymer

Light scattering studies on the crystalline morphology of stretched poly(ethylene 2,6-naphthalate) film

Joo Young Nam [a], Mari Fukuoka [b], Hiromu Saito [b,*], Takashi Inoue [c]

[a] Department of Organic and Polymeric Materials, Tokyo Institute of Technology, 2-12-1 Ookayama, Meguro-ku, Tokyo 152-8552, Japan
[b] Department of Organic and Polymer Materials Chemistry, Tokyo University of Agriculture and Technology, 2-24-16 Nakacho, Koganei-shi, Tokyo 184-8588, Japan
[c] Department of Polymer Science and Technology, Yamagata University, Jonan, Yonezawa-shi, Yamagata 992-8510, Japan

Received 27 March 2006; accepted 19 February 2007
Available online 22 February 2007

Abstract

The crystalline morphology of poly(ethylene 2,6-naphthalate) (PEN) film obtained by uniaxial stretching at 145 °C ($T_g + 25$ °C) was investigated by use of a light scattering photometer equipped with a CCD camera system. The Hv scattering showed a symmetric, circular pattern at a low stretch ratio of $\lambda < 3$. The intensity profile became sharper with an increase in λ, suggesting that anisotropic crystal rods are randomly assembled and that the length of the rods increases with λ. At a high stretch ratio of $\lambda \geq 3$, a double-cross-type pattern consisting of a broad rod-like pattern and sharp cross streaks was observed. The rod-like pattern became smaller and the streaks became sharper with an increase in λ. By the model calculation of the scattering pattern, the double-cross-type pattern is explained by the stacking of anisotropic crystal rods oriented in the stretch direction. As λ increases, the thickness of the rods and the number per stack increase, and the stacks and rods are slightly oriented in the stretch direction. The change in the wide angle X-ray diffraction pattern suggested that the ordering of the molecular chain in the crystal rods increases with increasing λ.

Keywords: Poly(ethylene 2,6-naphthalate); Light scattering; Crystallization

1. Introduction

The stretching of polymers causes the chains to align in the stretch direction and induces crystallization. Stretching plays an important role in providing the excellent inherent properties of polymers to the final products as well as some additional characteristics associated with their use. Hence, studies on the structural changes of crystalline polymers during stretching are not only of academic interest but also of industrial significance because the basic research on structural control is helpful in producing excellent manufactured goods.

Poly(ethylene 2,6-naphthalate) (PEN) is a slow crystallizing polymer that can be formed into an amorphous state from the melt by quenching and can be crystallized from the melt by slow cooling or by stretching at a temperature between the temperatures of glass transition and cold crystallization [1]. The chemical structure of PEN is explained by replacing the benzene ring in poly(ethylene terephthalate) (PET) with a naphthalene ring [2]. Owing to the stiffness of the molecular chain than that of PET, PEN is used as a high-performance polymer which has good heat resistance, low permeability, high strength, high modulus, and excellent dielectric properties [3–5]. Characteristic crystallization and stretching behaviors were observed in PEN, i.e., PEN has two different crystal modifications while PET has only one [6–8]. PEN also shows necking behavior by stretching from the amorphous state above the glass transition temperature T_g due to the highly cooperative orientation of the naphthalene planes parallel to the surface of the film [9,10]. Owing to both academic interest and industrial significance, many studies have been reported on the changes in structure and formation during stretching

* Corresponding author. Tel./fax: +81 42 388 7294.
E-mail address: hsaitou@cc.tuat.ac.jp (H. Saito).

0032-3861/$ - see front matter © 2007 Elsevier Ltd. All rights reserved.
doi:10.1016/j.polymer.2007.02.051

[1,11–22]. However, the structure of stretched PEN is not detectable on a nanometer level by small angle X-ray scattering measurement. Thus, the studies on stretched PEN are limited to the crystalline structure estimated by wide angle X-ray diffraction (WAXD); details of the change of structure during the stretching have not been clarified.

The light scattering method is sufficient to characterize the structure on a scale from a hundred nanometers to several micrometers [23]. Recently, Okamoto, Ishihara and Cakmak et al. found that the double-cross-type pattern consisting of a rod-like pattern and cross streaks appeared in stretched PEN films through their Hv light scattering studies [16,21,22], suggesting that the structure on a scale from a hundred nanometers to several micrometers is obtained during the stretching. In this paper, we prepare stretched PEN films by uniaxial stretching at different stretch ratios at $T_g + 25$ °C, and investigate the Hv scattering pattern of the stretched PEN by using a CCD camera system. The change of the structure during the stretching is quantitatively discussed by the model calculation of a series of characteristic Hv scattering patterns. For deeper understanding of the structural change, the WAXD results are also presented.

2. Experimental

The amorphous PEN film was supplied by Teijin Co. Ltd. The film specimen was 100 μm thick. It was cut into a rectangle of 50 mm × 5 mm. The film specimen was uniaxially stretched to the desired stretch ratios λ at 145 °C ($T_g + 25$ °C) in a hot chamber by using a hand-operated stretch machine. Here the specimen was allowed to equilibrate at the stretching temperature for 1 min before being stretched in the chamber. In order to prevent the crystallization after the stretching, the stretched specimen was quenched by being immersed into an ice water bath immediately after the stretching.

A polarized He–Ne laser with a wavelength of 632.8 nm was applied vertically to the stretched film specimen thus obtained. The scattered light was passed through an analyzer and then onto a highly sensitive charge-coupled device (CCD) camera with a 512 × 512 pixel sensor of dimensions 13.3 × 8.8 mm (Princeton Instruments, Inc., TE/CDD-512-TKM-1). We employed Hv geometry in which the optical axis of the analyzer was set perpendicularly to that of the polarizer. The stretch direction of the film specimen was vertical to the optical axis of the analyzer. The input data from the CCD camera were digitized by an ST-13X controller and stored in a personal computer for further analysis [23–25].

The model calculation for light scattering patterns was performed by Mathematica software (Wolfram Research, Inc.).

The crystalline structure was also observed under polarized optical microscope (Olympus BH-2). DSC thermogram was measured by using Seiko Instruments Exster 6200 calibrated with standard indium. A WAXD pattern of the specimen was observed by an X-ray diffraction apparatus (Rigaku-Denki RU-H3R) using a Fuji Film HR-V imaging plate. The radiation from the copper anode was reflected from a Ni-filtered Cu Kα radiation with a wavelength of 0.154 nm. The generator was operated at 50 kV and 100 mA.

3. Results and discussion

Amorphous PEN film was uniaxially stretched at 145 °C ($T_g + 25$ °C). Fig. 1 shows the Hv light scattering patterns of the stretched PEN films obtained at different stretch ratios λ. Here, the stretch direction SD was vertical to the optical axis of the analyzer A and parallel to that of the polarizer P. Although the film specimens were transparent, characteristic Hv scattering patterns were obtained. The Hv scattering showed a symmetric, circular pattern at a low stretch ratio of $\lambda < 3$. In contrast, a double-cross-type pattern consisting of a broad rod-like pattern and sharp cross streaks was observed at an angle of 25° by stretching the material to a high stretch ratio of $\lambda \geq 3$. The azimuthal angle of the rod pattern decreased from 49° to 42°, and that of the streaks decreased from 10° to 2° with an increase in λ from 3 to 5. The appearance of the Hv light scattering suggests the crystallization of the amorphous PEN by stretching at 145 °C [26], and the change in the scattering pattern with λ indicates a change in the crystalline morphology during the stretching.

Fig. 2a shows the one-dimensional intensity profile for the symmetric, circular pattern indicated in Fig. 1a and b. The intensity is strongest in the center and decreases monotonically with an increase in the scattering angle θ. The intensity increases and the profile becomes sharper as the stretch ratio increases. The appearance of the circular scattering pattern and the monotonous decrease of the intensity with θ suggest that anisotropic rods are randomly assembled.

The light scattering pattern of the randomly assembled anisotropic rods is theoretically described by [28,29],

$$I_{Hv} = \rho_0^2 L^2 N_0 \int_0^{\pi} \delta^2 \sin^2(\alpha+\omega_0)\cos^2(\alpha+\omega_0) \times [\sin(kaL/2)/(kaL/2)]^2 d\alpha \quad (1)$$

Here, ρ_0 is the scattering power of a rod per unit length, L is the length of the rod, N_0 is the number of rods, k is $2\pi/\lambda'$ where λ' is the wavelength of light in the medium, δ is the optical anisotropy of the rod, α is the tilt angle of the rod, ω_0 is the angle between the direction of maximum polarizability and the longitudinal direction of the rod, $a = -\sin(\alpha+\mu)\sin\theta$ where μ and θ are the azimuthal angle and the scattering angle, respectively.

Fig. 2b shows the calculated Hv light scattering pattern for the randomly assembled rods obtained by Eq. (1). The symmetric, circular pattern is obtained when the length of the rod is less than 600 nm (Fig. 2b), while a rod-like pattern is obtained when the length of the rod is above 600 nm. As shown in Fig. 2c, the scattering intensity increases and the profile becomes sharper with an increase in the length and number of rods. These results suggest that anisotropic crystal rods having a length of less than 600 nm are developed and are randomly oriented by stretching the film at a low stretch ratio. The number and length of the crystal rods increase as the stretch ratio increases.

As shown in Fig. 1c–e, a double-cross-type pattern is observed for the specimen stretched at high stretch ratio of $\lambda \geq 3$. A broad rod-like pattern appeared in the wide angle region while a sharp cross streak appeared in the small angle

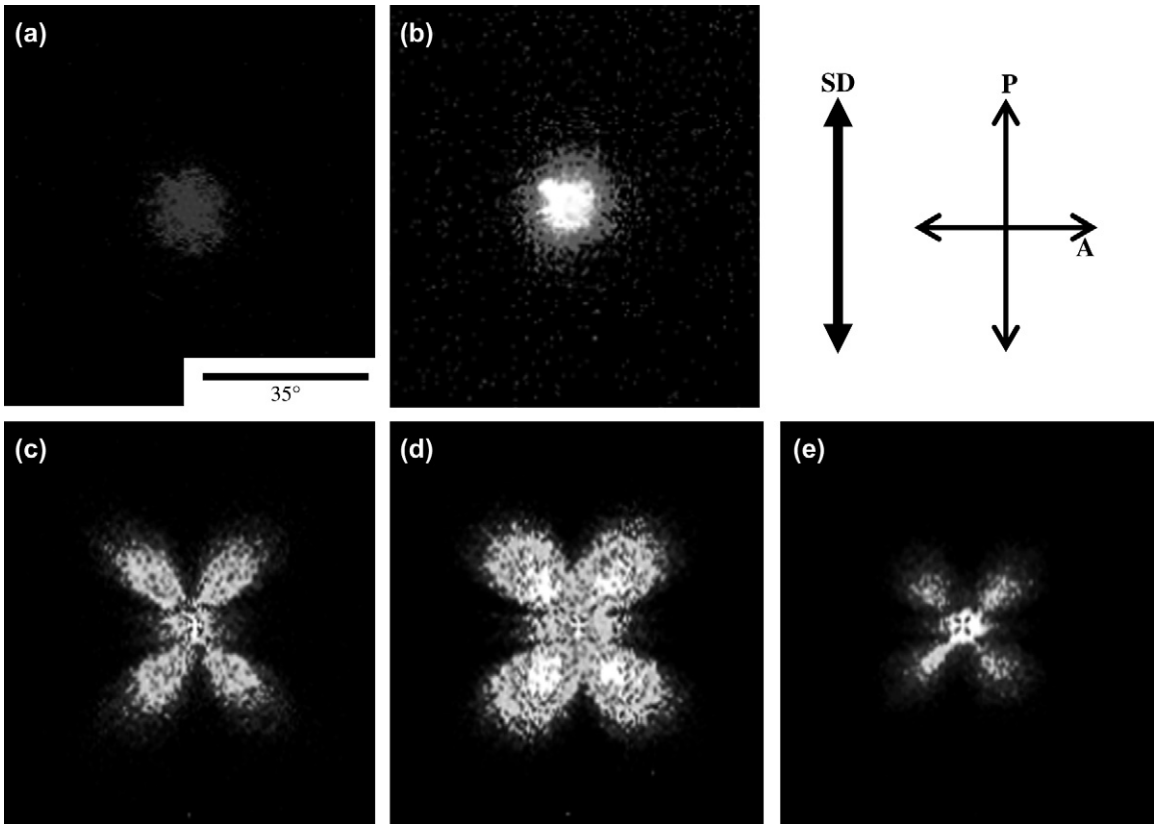

Fig. 1. Hv light scattering patterns of PEN film stretched at various values of λ: (a) $\lambda = 1.5$, (b) $\lambda = 2$, (c) $\lambda = 3$, (d) $\lambda = 4$, (e) $\lambda = 5$.

region. The scattering intensity increases as the stretch ratio increases. The cross streak pattern becomes sharper and the rod-like pattern becomes smaller as the stretch ratio increases.

A double-cross-type pattern can be explained by assuming that the stacked rods are oriented in the particular angle γ with respect to the direction of the stretch [30–32]. Fig. 3 is a schematic diagram of the stacked rods. We assumed that (1) the planar rods having length L and thickness D are stacked with a correlation length of X, (2) the rod has an optical anisotropy in a longitudinal direction and (3) the longitudinal direction of the rods is tilted at angle α with respect to the direction of the stretch. The Hv light scattering intensity for the stacked rods is described by applying the theory of small angle X-ray scattering for stacked lamellae by Blundell [33,34] and Hosemann [35]

$$I_{\mathrm{Hv}} = \mathrm{Re}\left\{ J - G^2 + \frac{1+F_x}{1-F_x}G^2 \right\} - \mathrm{Re}\left\{ \frac{2G^2F_x\left(1-F_x^N\right)}{N\left(1-F_x\right)^2} \right\} \quad (2)$$

$$F_x = |F|\exp[-2\pi i \sin\theta\cos(\mu-\gamma)\overline{X}/\lambda'] \quad (3)$$

$$|F| = \exp\left[-2\pi^2 \sin^2\theta\cos^2(\mu-\gamma)\sigma_x^2\overline{X}/\lambda'^2\right] \quad (4)$$

where μ is the azimuthal angle, γ is the oriented angle of the stacked rods, and λ' is the wavelength of light in the medium. The first term in the right-hand side of Eq. (2) primarily contributes to the first and higher order diffraction peaks; the second term gives the zero-order scattering.

Assuming that all rods have the same size without orientation fluctuation, J and G are given by [32]

$$J = (\vec{M}\cdot\vec{O})^2(DL)^2\frac{\sin^2\{\pi L\sin\theta\sin(\mu-\alpha)/\lambda'\}}{\{\pi L\sin\theta\sin(\mu-\alpha)/\lambda'\}^2} \times\frac{\sin^2\{\pi D\sin\theta\cos(\mu-\alpha)/\lambda'\}}{\{\pi D\sin\theta\cos(\mu-\alpha)/\lambda'\}^2} \quad (5)$$

$$G = (\vec{M}\cdot\vec{O})(DL)\frac{\sin\{\pi L\sin\theta\sin(\mu-\alpha)/\lambda'\}}{\pi L\sin\theta\sin(\mu-\alpha)/\lambda'} \times\frac{\sin\{\pi D\sin\theta\cos(\mu-\alpha)/\lambda'\}}{\pi D\sin\theta\cos(\mu-\alpha)/\lambda'} \quad (6)$$

where D and L are the mean thickness and mean length of the rod, respectively. $(M\cdot O)$ denotes the scalar product of the induced dipole moment M and the vector O along the direction of polarization of the analyzer for the horizontal polarization given by [32]

$$(\vec{M}\cdot\vec{O}) = \frac{\delta_0}{2}\cos\rho_2\sin\{2(\xi-\gamma)\}E_0 \quad (7)$$

$$\cos\rho_2 = \frac{\cos\theta}{\sqrt{\cos^2\theta+\sin^2\theta\sin^2\mu}} \quad (8)$$

where δ_0 is the anisotropy of the rods defined by $\alpha_1 - \alpha_2$ in which α_1 and α_2 are polarizabilities along and perpendicular to the optical axis, respectively, E_0 is the amplitude of an incident

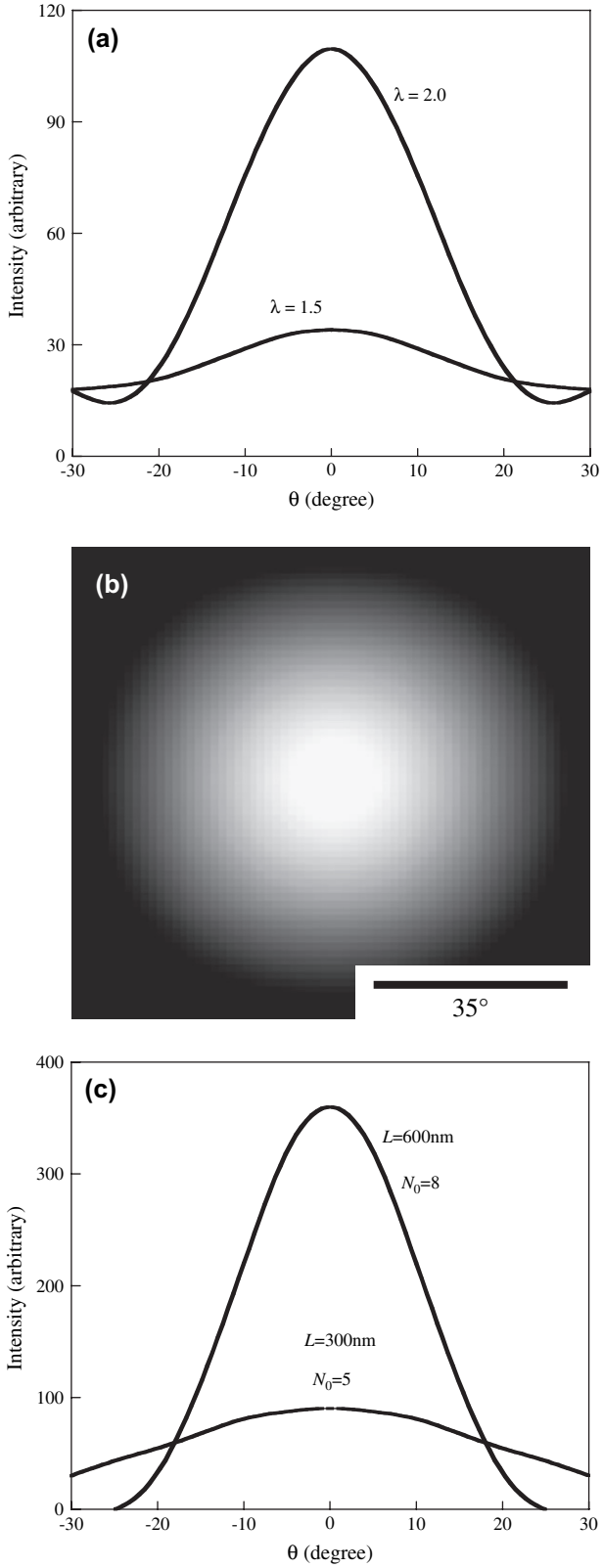

Fig. 2. Analyzing results for the symmetric, circular pattern shown in Fig. 1a and b: (a) one-dimensional intensity profiles for Fig. 1a ($\lambda = 1.5$) and b ($\lambda = 2$), (b) calculated Hv light scattering pattern obtained by assuming $L = 300$ nm and $N_0 = 5$, (c) calculated one-dimensional intensity profiles obtained by assuming various values of L and N_0.

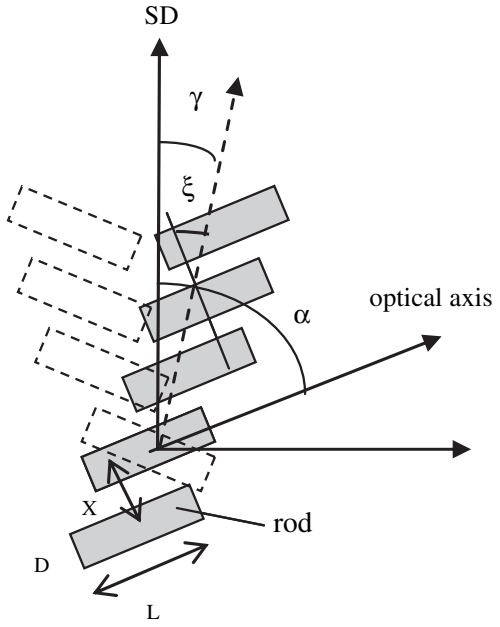

Fig. 3. Schematic diagram of the stacked rods with respect to the direction of stretching.

beam, and ξ is the orientation angle between the direction of stretch and the longitudinal direction of the rod.

Fig. 4 shows the calculated Hv light scattering patterns for various values of α and γ. The double-cross-type scattering pattern shown in Fig. 1c–e is reproduced by Eqs. (3)–(8). By assuming $D = 300$ nm and $L = 1500$ nm, the calculated pattern is obtained at a wide angle region of about 25°, as demonstrated in the experimental results shown in Fig. 1c–e. The azimuthal angle μ of the rod pattern decreases as α increases, while μ of the streaks increases as γ increases. As shown in Fig. 1c–e, the azimuthal angle of the rod-like pattern decreases from 49° to 42°, and that of the cross streaks decreases from 10° to 2° as the stretch ratio increases from 3 to 5. These results can be explained by assuming that α changes from 49° to 42° while γ changes from 10° to 2° as the stretch ratio increases. Thus, the stacked rods and the rods in the stack are oriented in the direction of the stretch as the stretch ratio increases.

Fig. 5 shows the calculated Hv light scattering patterns for various thicknesses D and lengths L of the rod. Here, we assumed that the stacked rods are oriented at angles $\gamma = \pm 10°$ and the rods are oriented at $\alpha = \pm 45°$, respectively, and that N is 15 and X is 1200 nm. The rod pattern becomes sharper and the intensity becomes stronger as L increases (Fig. 5a). The scattering angle of the rod pattern becomes smaller and the intensity becomes stronger as D increases (Fig. 5b). These results suggest that (1) the scattering pattern appearing at the wide angle region is attributed to the small size of the crystal rods, (2) the scattering angle depends on D and L, and (3) the contribution of L to the scattering is larger than that of D. The calculated results are in good agreement with the experimental results by assuming that L and D increase as the stretch ratio increases.

Fig. 6 shows the calculated Hv light scattering patterns for various numbers of rods in the stack N and long period X. Here, α and γ are assumed to be $\pm 45°$ and $\pm 10°$, respectively.

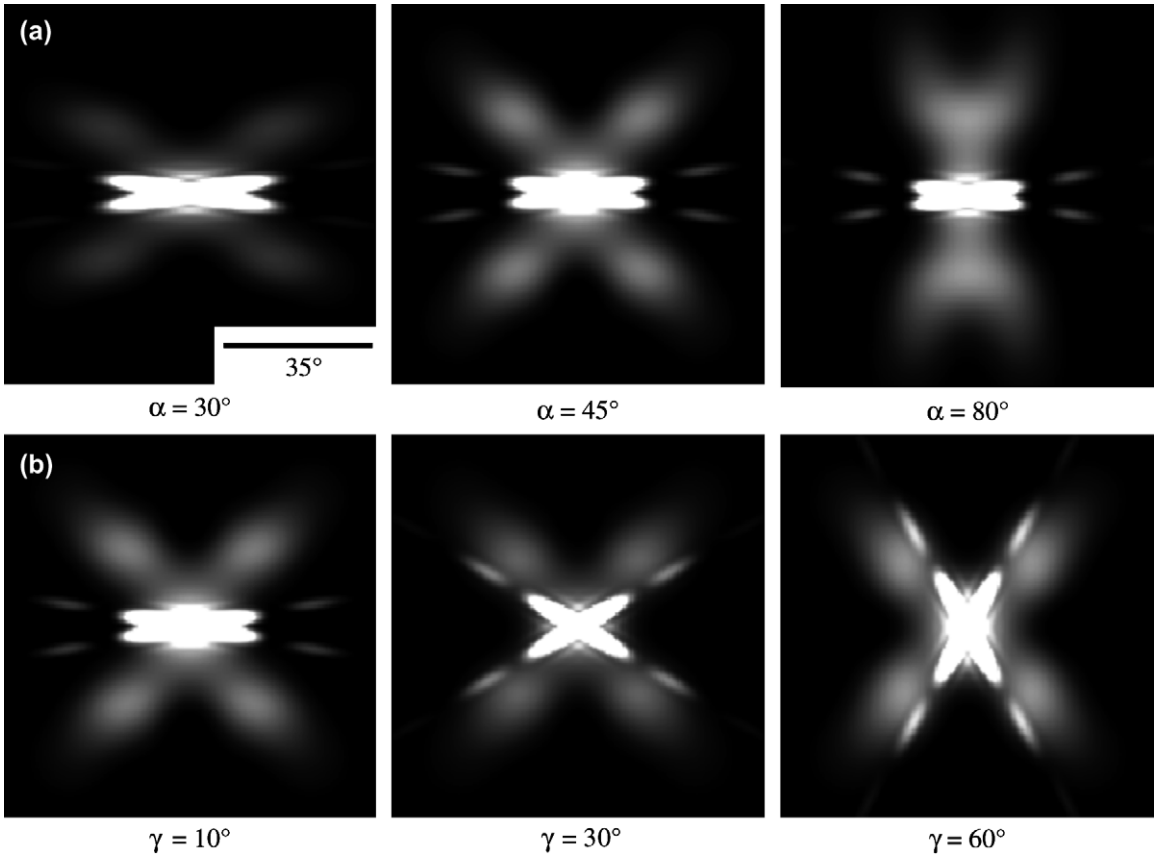

Fig. 4. Calculated Hv light scattering patterns for various values of (a) α and (b) γ by assuming $D = 300$ nm, $L = 1500$ nm, $N = 10$, and $X = 1200$ nm.

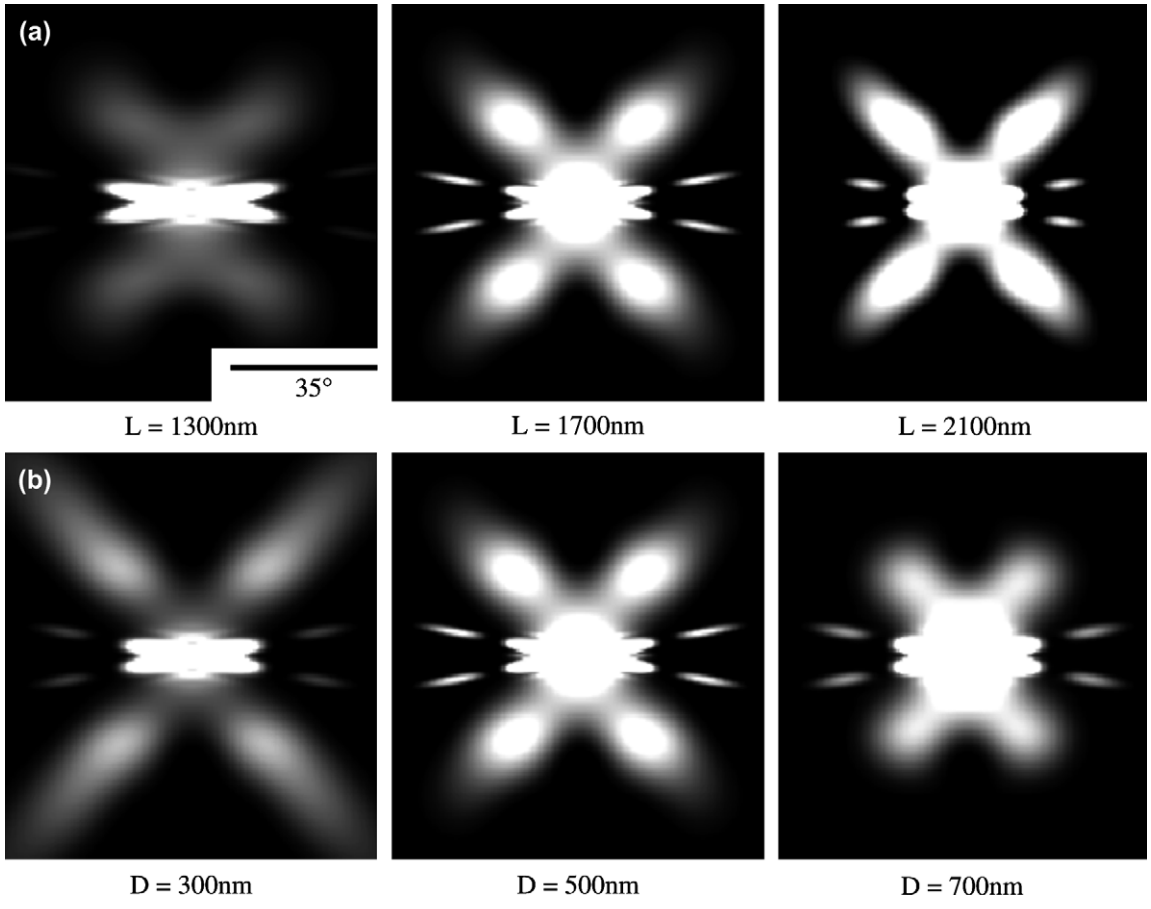

Fig. 5. Calculated Hv light scattering patterns for various values of (a) L and (b) D by assuming $\gamma = \pm 10°$, $\alpha = \pm 45°$, $N = 15$, and $X = 1200$ nm.

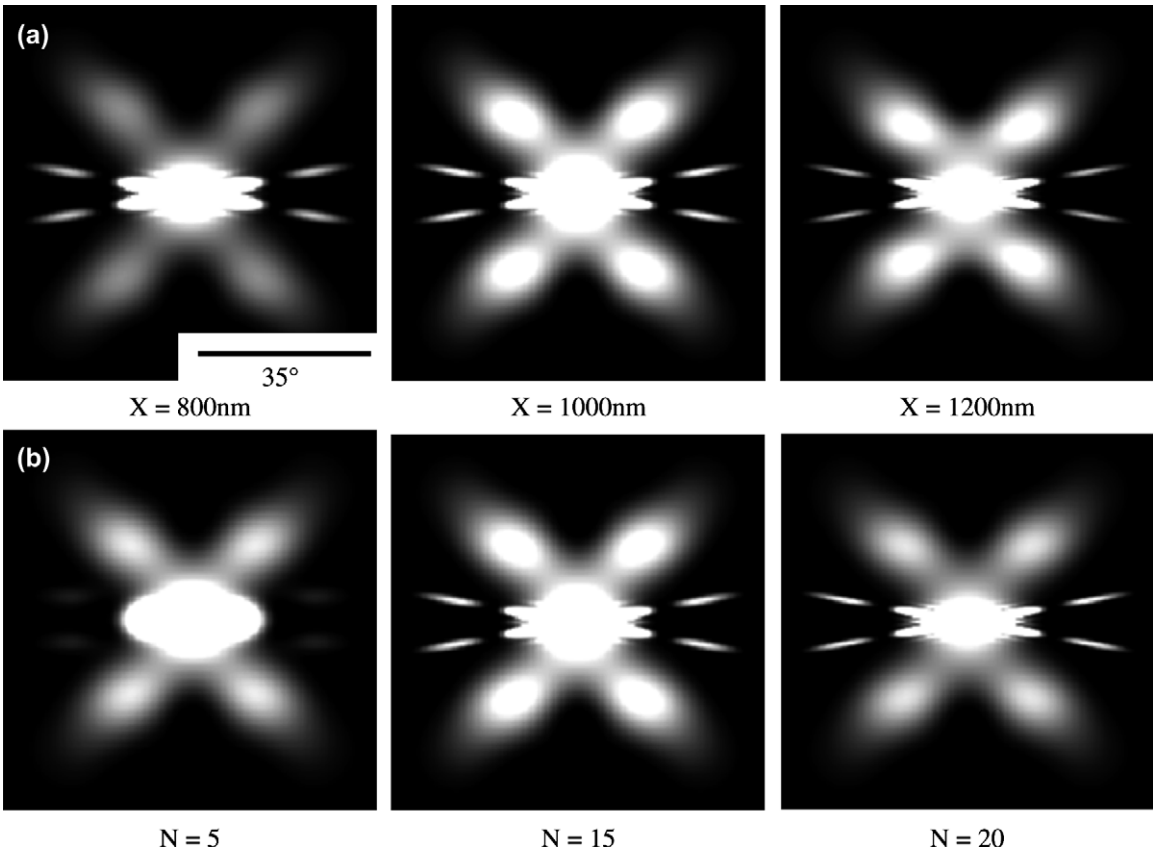

Fig. 6. Calculated Hv light scattering patterns for various values of (a) X and (b) N by assuming $\gamma = \pm 10^\circ$, $\alpha = \pm 45^\circ$, $D = 300$ nm, and $L = 1500$ nm.

Table 1
Intensity ratio I_r/I_s and crystallinity X_c

Experimental			Calculation	
λ	(I_r/I_s)	X_c[a]	(I_r/I_s)	X_c[b]
3	4.75	22.7	4.29	17.6
4	5.60	34.7	5.42	33.3
5	5.62	48.3	5.80	50.0

[a] The degree of crystallinity estimated by DSC.
[b] The degree of crystallinity estimated by D/X.

The streak pattern becomes sharper and the intensity increases as N increases. As demonstrated in Fig. 1c–e, the streak pattern becomes sharper and the intensity increases as the stretch ratio increases. Thus, the results suggest that the number of crystal rods in the stack increases as the stretch ratio increases.

Since the intensity of the rod pattern I_r depends on the rod size while the intensity of the streak I_s depends on the number of the rod and long period, I_r/I_s at 10° and the crystallinity of the experimental results were compared with those of the calculated ones to obtain the desirable parameters (Table 1). As shown in Fig. 7,

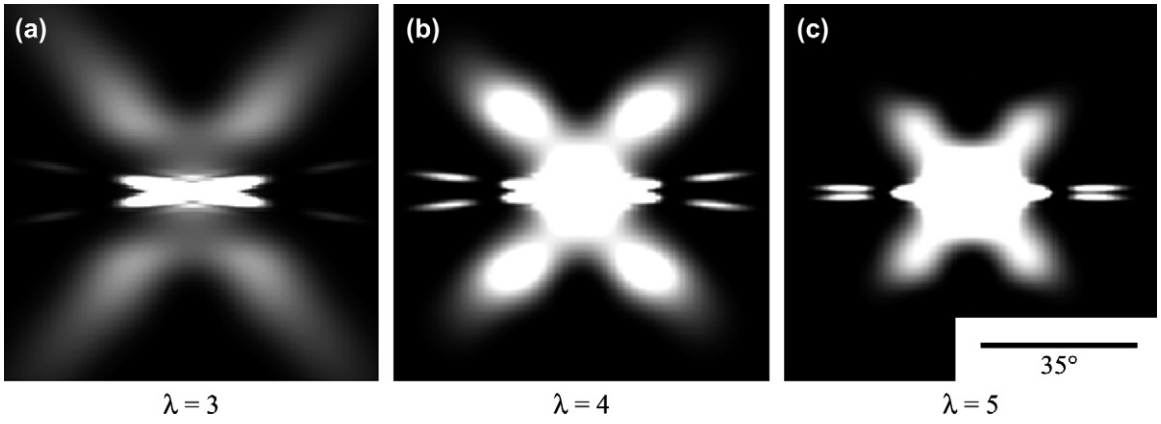

Fig. 7. Calculated Hv light scattering patterns corresponding to Fig. 1c–e obtained by desirable parameters: (a) $N = 10$, $L = 1500$ nm, $D = 300$ nm, $X = 1700$ nm, $\alpha = \pm 49^\circ$, $\gamma = \pm 10^\circ$; (b) $N = 15$, $L = 1700$ nm, $D = 500$ nm, $X = 1500$ nm, $\alpha = \pm 45^\circ$, $\gamma = \pm 6^\circ$; (c) $N = 20$, $L = 2000$ nm, $D = 700$ nm, $X = 1400$ nm, $\alpha = \pm 42^\circ$, $\gamma = \pm 2^\circ$.

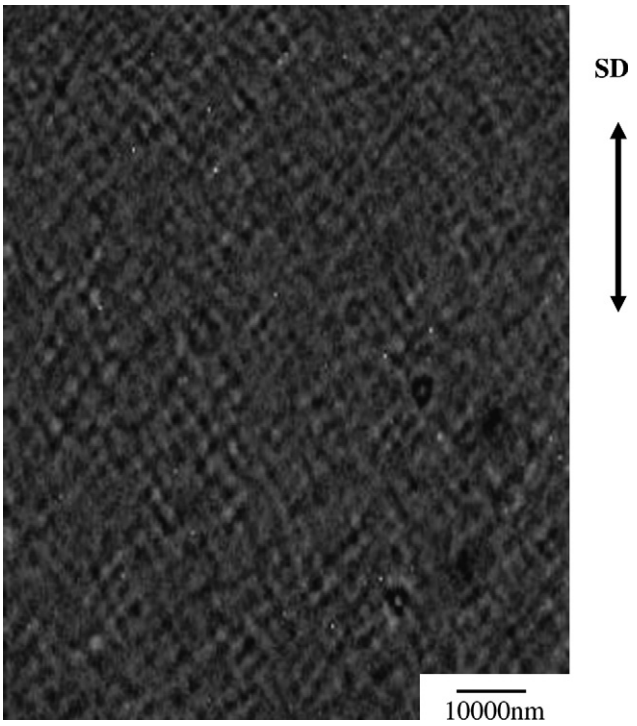

Fig. 8. Polarizing optical micrograph of PEN film stretched at $\lambda = 5$.

the experimental Hv light scattering patterns shown in Fig. 1c–e are reproduced by using the desirable parameters of α, γ, L, D, and X indicated in the legends of Fig. 7a–c. According to the calculated results indicated in Table 1, the thickness of the crystal rods is about 500 nm and the long period is about 1500 nm. This might imply that the crystal rod is too large to be detected by SAXS measurement. The existence of the stacked rods having a size of about 1000 nm was confirmed by the polarizing optical micrograph shown in Fig. 8.

Fig. 9 is a schematic illustration of the evolution of the crystalline structure during the stretching of the amorphous PEN film. At a low stretch ratio, anisotropic crystal rods are developed and are randomly arranged. When the stretch ratio is above 3, the crystal rods are stacked and are oriented in the direction of the stretch. As the stretch ratio increases, the thickness of the rods and the number of the rods in the stack increase, and the stacks and the rods are slightly oriented in the direction of the stretch.

The melting temperature of the stretched PEN ($\lambda = 5$) was 273 °C while that of the unstretched PEN was 270 °C. Since the melting temperature is related to the lamellar size, i.e., melting temperature increases with increasing lamellar thickness [36,37], the results suggest that the lamellar size of the stretched PEN is close to that of the unstretched PEN. According to Lee et al. [8], lamellar size of unstretched PEN is several ten nanometers. Thus the size of the crystal rod is much larger than that of the lamella. This may imply that the crystal rod is not uniform crystal but it consists of amorphous region and crystalline lamellae having a size of several ten nanometers, as schematically illustrated in Fig. 9.

Fig. 10 shows the WAXD patterns of the stretched PEN films. The WAXD patterns for $\lambda = 3$ and $\lambda = 4$ are diffusive and are almost same to amorphous halo (Fig. 10a and b), suggesting poor crystalline ordering in the crystal rods. The intensity of the halo concentrates toward the equator, indicating that the molecular chains are preferentially oriented in the direction of the stretch [9,13,20]. On the other hand, spot-like crystalline diffractions of the α form are seen at $\lambda = 5$ (Fig. 10c), suggesting good crystalline ordering in the crystal rods and large chain orientation. Thus, the ordering of the molecular chain in the crystal rod and the chain orientation increase with increasing λ, as schematically illustrated in Fig. 9.

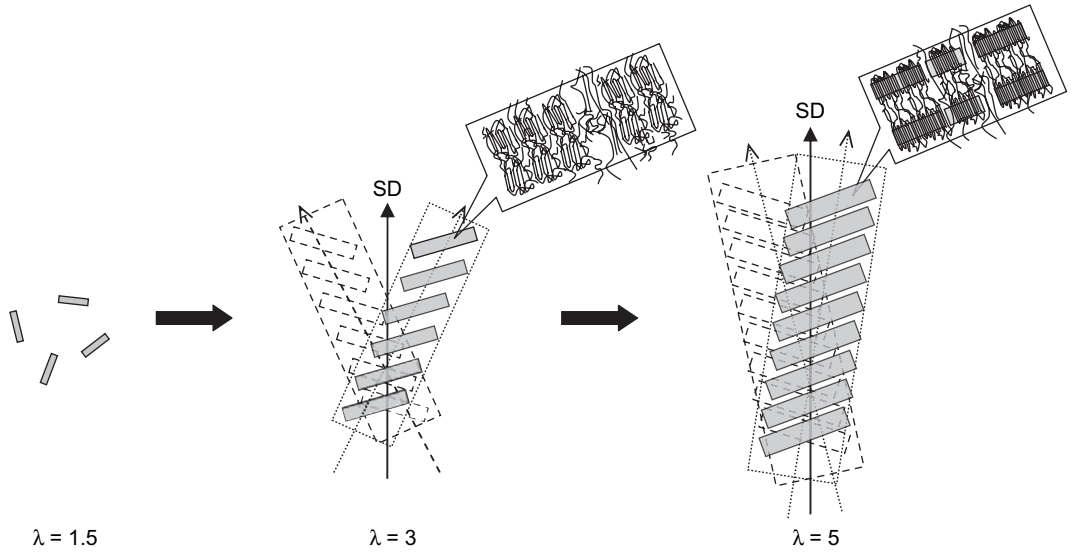

Fig. 9. Schematic diagram of the evolution of the crystalline structure during the stretching of PEN film.

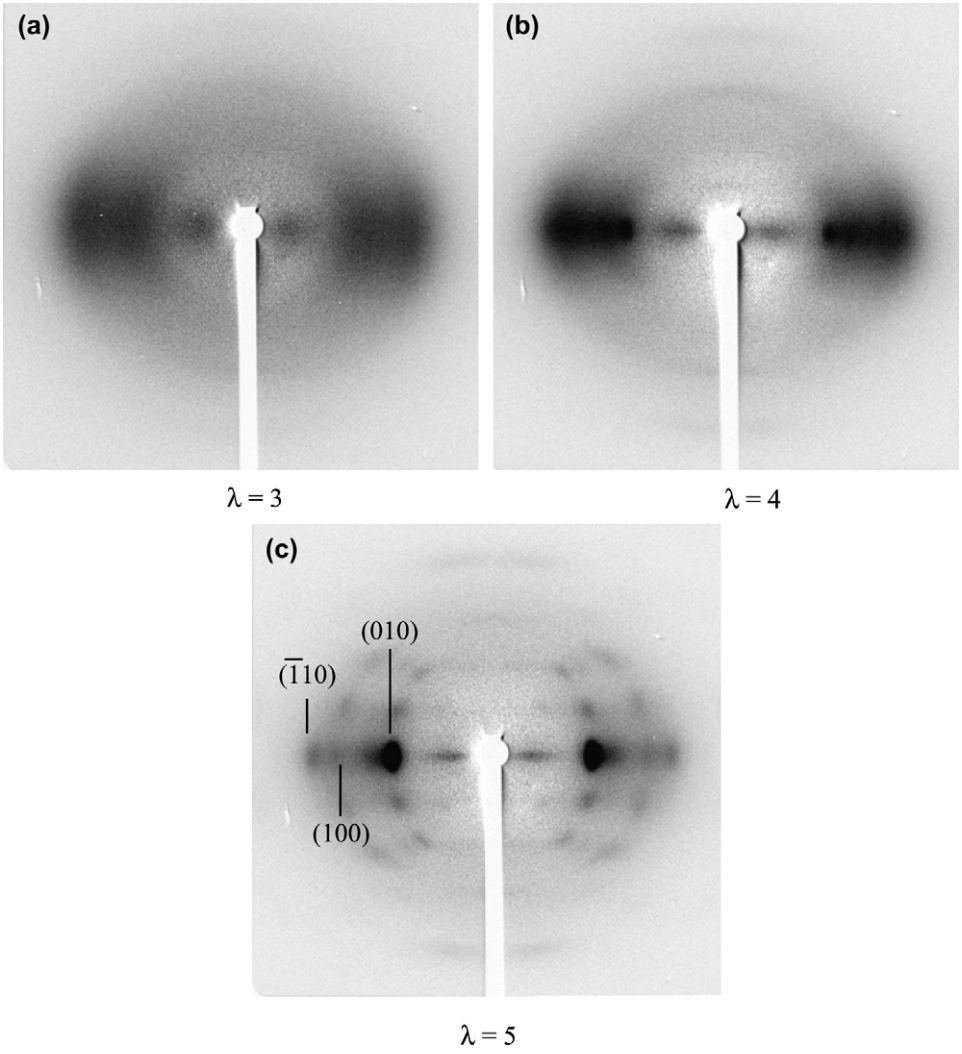

Fig. 10. WAXD pattern of PEN film stretched at $\lambda = 3$ and $\lambda = 5$.

4. Conclusion

Changes in the Hv light scattering patterns of stretched PEN films with stretch ratios and model calculations for the scattering patterns revealed the development of the structure during the stretching. At a low stretch ratio of $\lambda < 3$, anisotropic crystal rods are developed and are randomly assembled. The number and length of the crystal rods increase as the stretch ratio increases, and the rods are stacked at $\lambda = 3$. As the stretch ratio increases, the thickness of the rods and the number of rods per stack increase, and the stacks and rods are slightly oriented in the direction of the stretch.

References

[1] Schoukens G, Samyn P, Maddens S, Van Audenaerde T. J Appl Polym Sci 2003;87:1462.
[2] Cook JG, Huggill HPW, Lowe FR. Br Patent GB604073; 1948.
[3] Cheng SZD, Wunderlich B. Macromolecules 1988;21:789.
[4] Nakamae K, Nishino T, Tada K, Kanamoto T, Ito M. Polymer 1993;34:3322.
[5] Hardy L, Stevenson I, Boiteux G, Seytre G, Schöhnhals A. Polymer 2001;42:5679.
[6] Buchner S, Wiswe D, Zachmann HG. Polymer 1989;30:480.
[7] Guo M, Zachmann HG. Macromol Chem Phys 1998;199:1185.
[8] Lee WD, Yoo ES, Im SS. Polymer 2003;44:6617.
[9] Cakmak M, Lee SW. Polymer 1995;36:4039.
[10] Murakami S, Yamakawa M, Tsuji M, Kohjiya K. Polymer 1996;37:3945.
[11] Cakmak M, Wang YD, Simhambhatla M. Polym Eng Sci 1990;30:721.
[12] Ito M, Honda K, Kanamoto T. J Appl Polym Sci 1992;46:1013.
[13] Murakami S, Nishikawa Y, Tsuji M, Kawaguchi A, Kohjiya S, Cakmak M. Polymer 1995;36:291.
[14] Miyata K, Kikutani T, Okui N. J Appl Polym Sci 1997;65:1415.
[15] Cakmak M, Kim JC. J Appl Polym Sci 1997;64:729.
[16] Okamoto M, Kubo H, Kotaka T. Macromolecules 1998;31:4223.
[17] Yoshioka T, Tsuji M, Kawahara Y, Kohjiya S. Polymer 2003;44:7997.
[18] Schoukens G. Polymer 1999;40:5637.
[19] Yoon WJ, Myung HS, Kim BC, Im SS. Polymer 2000;41:4933.
[20] Wu G, Li Q, Cuculo JA. Polymer 2000;41:8139.
[21] Galay J, Cakmak M. J Polym Sci Part B Polym Phys 2001;39:1147.
[22] Ishihara H, Gotoh M, Yoshihara N, Okudaira T. J Jpn Soc Polym Process 2002;14:378.
[23] Saito H, Inoue T. In: Simon GP, editor. Polymer characterization techniques and their application to blends, light and X-ray scatterings. Washington, DC: Oxford University Press; 2003. p. 313–45.
[24] Lee CH, Saito H, Inoue T. Macromolecules 1993;24:8096.

[25] Tsuburaya M, Saito H. Polymer 2004;45:1027.
[26] The crystallization did not occur before the stretching because the cold crystallization of PEN is quite slow; e.g., the induction period of the crystallization is above 10 min at 145 °C [27]. The crystallization is induced by stretching and occurs during the stretching [10,11,13,18].
[27] Nogales A, Ezquerra TA, Denchev Z, Baltá-Calleja FJ. Polymer 2001;42:5711.
[28] Samuels RJ. J Polym Sci Part A-2 1969;7:1197.
[29] Rhodes MB, Stein RS. J Polym Sci Part A-2 1969;7:1539.
[30] Hashimoto T, Todo A, Kawai H. Polym J 1978;10:521.
[31] Matsuo M, Tamada M, Terada T, Sawatari C, Niwa M. Macromolecules 1982;15:985.
[32] Sawatari C, Iida M, Matsuo M. Macromolecules 1984;17:1765.
[33] Blundell DJ. Acta Crystallogr A 1970;26:472.
[34] Blundell DJ. Acta Crystallogr A 1970;26:476.
[35] Hosemann R. Z Phys 1949;127:16.
[36] Wunderlich B. Macromolecular physics: crystal melting, vol. 3. New York: Academic Press; 1980.
[37] Bassett DC. Principles of polymer morphology. Cambridge: Cambridge University Press; 1981.